

Benzene and Tropylium Metal Complexes. Intra- and Intermolecular Interaction Evidenced by Vibrational Analysis: The Blue-Shift Hydrogen Bond

Pier Luigi Stanghellini,^{*,†} Eliano Diana,[‡] Aldo Arrais,[‡] Andrea Rossin,^{‡,§} and Sidney F. A. Kettle[⊥]

Dipartimento di Scienze e Tecnologie Avanzate, Università del Piemonte Orientale, via V. Bellini 25/G, 13100 Alessandria, Italy, Dipartimento di Chimica I.F.M., Università di Torino, via P. Giuria 7, 10125 Torino, Italy, and School of Chemical Sciences, University of East Anglia, Norwich, NR4 7TJ, Great Britain

Received May 18, 2006

Vibrational IR and Raman spectra of several organometallic complexes of benzene and tropylium have been investigated. Comparisons between the vibrational features of free and coordinated ligands and between solution and solid-state spectra of the complexes have been performed. Similar sets of bands observed in the typical diagnostic regions suggest a weak kinematic coupling between the ligand vibrational modes. The high sensitivity of the frequency of the vibrations to electron charge density distributed throughout the complexes provides evidence of the intermolecular interactions characterizing the solid-state architecture. Noteworthy are the different types of C–H···X hydrogen bond, displaying both the blue- and red-shift of the CH stretching vibrations.

Introduction

The vibrational patterns (IR and Raman spectra) subtended by a C_nH_n ring bonded to a metal atom are, at first sight, very complicated. An example is shown in Figure 1.

The majority of the bands are associated with vibrations of the organic rings. If the spectra are to be interpreted in terms of the bond properties of the system (and, less expected, but equally important for crystalline samples, information on intermolecular interactions in the solid state), a complete and accurate vibrational analysis appears essential. Such an analysis requires the accurate assignment of the normal modes, often necessitating selective isotopic labeling, as the basis of a detailed force constant and energy distribution calculation. Not surprisingly, the use of the vibrational spectra simply as fingerprints of a complex is commonplace.

Some years ago we reported a study on the vibrations of the cyclopentadienyl ring bonded to a metal atom. The species covered were simple ionic complexes $[Cp^-]M^+$, covalent complexes with a simple Cp–M unit as in $CpM(CO)_n$, bimetallic and cluster systems, and, finally, metallocene Cp_2M complexes.¹

We demonstrated that, despite these different structures, the Cp ring gives rise to very similar sets of bands in appropriate spectral regions. This requires a weakness of kinematic coupling between modes with the same symmetry but different assignments. Such a weakness has been found in several normal coordinate analysis (NCA) and by density-functional theory (DFT) calculations.²

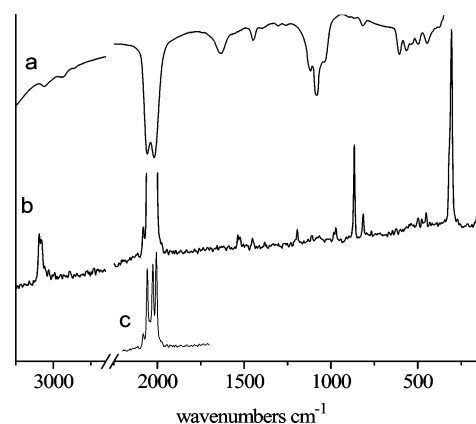


Figure 1. Solid-state infrared (a, KBr pellet) and Raman (b, c, crystal) spectra of the $[TpCr(CO)_3]^+[BF_4]^-$ complex.

It is evidently an acceptable approximation to consider many vibrational modes as localized. This places on a secure basis the commonplace division into different and well-localized spectral regions: C–H stretches, C–C stretches, C–C–H bends, and so on. Analysis of the bands in terms of both frequency and intensity, region by region, provided data on such topics as metal–ring bonding and the charge distribution within the ring. In the present paper we extend this work to metal complexes with either a C_6H_6 ring (benzene, Bz) or a C_7H_7 ring (tropylium, Tp). The complexes we have studied have the

* To whom correspondence should be addressed. E-mail: pierluigi.stanghellini@mfu.unipmn.it.

[†] Università del Piemonte Orientale.

[‡] Università di Torino.

[§] Current address: ICCOM-CNR, Area di Ricerca CNR di Firenze, via Madonna del Piano, 50019 Sesto Fiorentino (Firenze), Italy.

[⊥] University of East Anglia.

(1) (a) Diana, E.; Rossetti, R.; Stanghellini, P. L.; Kettle, S. F. A. *Inorg. Chem.* **1997**, *36*, 382. (b) Stanghellini, P. L.; Diana, E.; Boccaleri, E.; Rossetti, R. *J. Organomet. Chem.* **2000**, *593*, 36.

(2) (a) Aleksanyan, V. T. In *Vibrational spectra and structure*; Durig, J. R., Ed.; Elsevier Publ.: Amsterdam, 1982; Vol. 11, pp 107–167. (b) Bérces, A.; Ziegler, T.; Fan, L. *J. Phys. Chem.* **1994**, *98*, 1584. (c) Brunvoll, J.; Cyvin, S. J.; Schaefer, L. *J. Organomet. Chem.* **1971**, *27*, 69. (d) Schaefer, L.; Southern, J. F.; Cyvin, S. J. *Spectrochim. Acta, Part A* **1971**, *27*, 1083. (e) Brunvoll, J.; Cyvin, S. J.; Schaefer, L. *J. Organomet. Chem.* **1972**, *36*, 143. (f) Adams, D. M.; Christopher, R. E.; Stevens, D. C. *Inorg. Chem.* **1975**, *14*, 1562. (g) Schaefer, L.; Brunvoll, J.; Cyvin, S. J. In *Molecular Structural Vibrations*; Cyvin, S. J., Ed.; Elsevier: Amsterdam, 1972; pp 272–282. (h) Ketkov, S.; Selzle, H.; Schlag, E. *J. Chem. Phys.* **2004**, *121*, 149. (i) Bérces, A.; Ziegler, T. *J. Phys. Chem.* **1994**, *98*, 13233–13242.

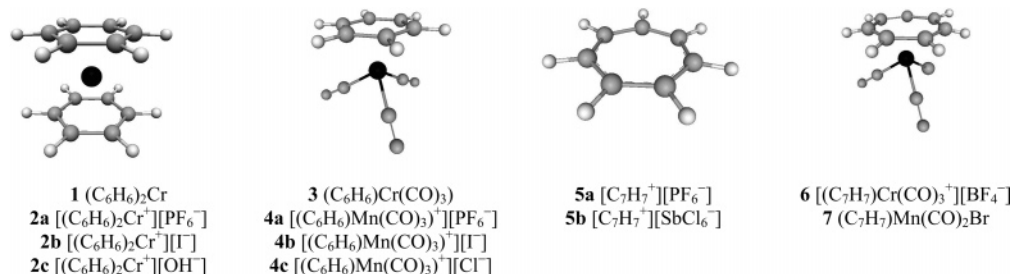


Figure 2. Schematic structures of the complexes.

structures illustrated in Figure 2. Some of these (**1**, **2**, **3**, **5**) are well-known, completely characterized complexes, and others (**6**) require deeper and more up-to-date insights into their vibrational properties. Yet others (**4**, **7**) are reported here for the first time. For none have the main vibrational features been compared; neither have the spectra in solution been compared with those in the solid state. In remedying this defect, we have obtained new and clear examples in an area that is currently of great interest in the field of the intermolecular chemical-physical properties of complex systems, the so-called blue-shift hydrogen bond.

Experimental Part

Reactants and Solvents. All manipulation were performed by standard Schlenk techniques under a nitrogen atmosphere. All of the basic reactants (aluminum powder, anhydrous $CrCl_3$, anhydrous $AlCl_3$, sodium dithionite, potassium iodide, $Mo(CO)_6$, $Mn_2(CO)_{10}$, $HClO_4$, $Cr(CO)_6$, trityl fluoroborate, lithium bromide, perchloric acid, sodium amide, and anhydrous iron(II) chloride) were purchased from Aldrich; alumina and silica gel TLC plates were from Merck.

Solvents were purified by standard methods. Benzene (Carlo Erba) and diglyme (Aldrich) were dried and distilled over sodium. CH_3CN (Carlo Erba) was purified by percolation through activated Al_2O_3 and subsequent distillation from P_2O_5 . Cycloheptatriene (Aldrich) was distilled before use. THF (Riedel) was distilled over sodium-benzophenone before use. CH_2Cl_2 , CCl_4 , acetone, petroleum ether, and *n*-hexane (Riedel) were degassed by standard techniques.

Complexes. Complexes **1**, **3**, and **5a** were purchased from Aldrich. Complex **1** was purified by sublimation before recording the spectra; complexes **2a**,³ **2b**,⁴ and **2c**⁵ were synthesized by the known procedure. Complex **4c** and the precursor $Mn(CO)_5Cl$ were prepared using well-known methods.⁶ The gaseous chlorine needed for the synthesis of the latter was generated by reaction of a solution of potassium permanganate in sulfuric acid with solid sodium chloride.

The complexes **4a** and **4b** were obtained from **4c** by metathesis reaction with KPF_6 and KI , respectively. The complex **5b** was synthesized according to the literature.⁷ The complex **6** was synthesized by treating the cycloheptatriene complex, prepared according to Wilkinson's procedure,⁸ with trityl fluoroborate.⁹ Compound **7** is obtained by reacting complex **6** with lithium bromide in acetone.¹⁰

(3) Grepioni, F.; Cojazzi, G.; Draper, S. M.; Scully, N.; Braga, D. *Organometallics* **1998**, *17*, 296.

(4) Morosin, B. *Acta Crystallogr.* **1974**, *B30*, 838.

(5) Braga, D.; Costa, A. L.; Grepioni, F.; Scaccianoce, L.; Tagliavini, E. *Organometallics* **1996**, *15*, 1084.

(6) Winkhaus, G.; Pratt, L.; Wilkinson, G. *J. Chem. Soc.* **1961**, 3807.

(7) Bryce-Smith, D.; Perkins, N. A. *J. Chem. Soc.* **1962**, 1339.

(8) Abel, E. W.; Bennett, M. A.; Burton, R.; Wilkinson, G. *J. Am. Chem. Soc.* **1958**, *80*, 4559.

(9) Dauben, J., Jr.; Hunnen, L. R. *J. Chem. Soc., Chem. Commun.* **1958**, 5571.

(10) Bochmann, M.; Green, M.; Hirsch, H. P.; Stone, F. G. A. *J. Chem. Soc., Dalton Trans.* **1977**, 714.

Spectroscopic Measurements. The infrared spectra of the solid samples were recorded as KBr or CsI pellets, and those of the solution as thin films between KBr windows using a Bruker Equinox 55 FTIR (2 cm^{-1} resolution). Complex **1** was sublimed in a vacuum on a cooled KBr window. Raman spectra were recorded from the sample sealed in a glass capillary under an inert N_2 atmosphere with a Bruker RFS 100 spectrophotometer, with a Nd^{3+}/YAG laser at $1064\ \mu\text{m}$ and Ge-diode detector (laser powers 30–150 mw, 10 00–5 000 acquisition scans, res. 4 cm^{-1}).

Calculations. All the DFT calculations were performed with the Gaussian package (Gaussian 03, revision C.02).¹¹ We use the B3LYP hybrid functional with the 6-31G(d,p) basis set for the H, C, O atoms and the LANL2DZ ECP basis set for the transition metals. All the structures were optimized, and the harmonic vibrational frequencies were calculated.

Results and Discussion

(A) Benzene Complexes. Table 1 SI reports a list of the vibrational modes of the free and coordinated benzene ligand, assuming the idealized symmetry of the complexes. The correlations of symmetry modes with those of free benzene are clear. Modes of the $B_{2v}M$ complexes having the same origin are grouped together because the coupling between the two rings is usually very weak and the two bands resulting exhibit very close frequencies.

The spectra and their assignment are well established for the benzene molecule;¹² our particular concern is with the IR and Raman spectra of the solid,¹³ as this facilitates comparison with the solid-state spectra of the complexes. Of these, the vibrational spectra of complexes **1**¹⁴ and **3**¹⁵ have been well studied, whereas the data for the others are either old (**2**, **4**, **6**) or absent

(11) Frisch, M. J.; Trucks, G. W.; Schlegel, H. B.; Scuseria, G. E.; Robb, M. A.; Cheeseman, J. R.; Montgomery, J. A., Jr.; Vreven, T.; Kudin, K. N.; Burant, J. C.; Millam, J. M.; Iyengar, S. S.; Tomasi, J.; Barone, V.; Mennucci, B.; Cossi, M.; Scalmani, G.; Rega, N.; Petersson, G. A.; Nakatsuji, H.; Hada, M.; Ehara, M.; Toyota, K.; Fukuda, R.; Hasegawa, J.; Ishida, M.; Nakajima, T.; Honda, Y.; Kitao, O.; Nakai, H.; Klene, M.; Li, X.; Knox, J. E.; Hratchian, H. P.; Cross, J. B.; Bakken, V.; Adamo, C.; Jaramillo, J.; Gomperts, R.; Stratmann, R. E.; Yazyev, O.; Austin, A. J.; Cammi, R.; Pomelli, J.; Ochterski, W.; Ayala, P. Y.; Morokuma, K.; Voth, G. A.; Salvador, P.; Dannenberg, J. J.; Zakrzewski, V. G.; Dapprich, S.; Daniels, A. D.; Strain, M. C.; Farkas, O.; Malick, D. K.; Rabuck, A. D.; Raghavachari, K.; Foresman, J. B.; Ortiz, J. V.; Cui, Q.; Baboul, A. G.; Clifford, S.; Cioslowski, J.; Stefanov, B. B.; Liu, G.; Liashenko, A.; Piskorz, P.; Komaromi, I.; Martin, R. L.; Fox, D. J.; Keith, T.; Al-Laham, M. A.; Peng, C. Y.; Nanayakkara, A.; Challacombe, M.; Gill, P. M. W.; Johnson, B.; Chen, W.; Wong, M. W.; Gonzalez, C.; Pople, J. A. *Gaussian 03*, revision C.02; Gaussian, Inc.: Wallingford, CT, 2004.

(12) Herzberg, G. *Infrared and Raman Spectra of Polyatomic Molecules*; Van Nostrand Reinhold Company; New York, 1966.

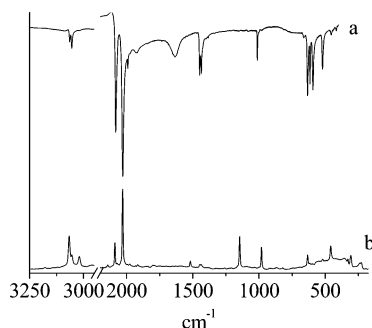
(13) Goodman, L.; Ozkabak, A. G.; Thakur, S. N. *J. Phys. Chem.* **1991**, *95*, 9044.

(14) (a) Snyder, R. G. *Spectrochim. Acta* **1959**, *10*, 807. (b) Cyvin, S. J.; Brunvoll, J.; Schäfer, L. *J. Chem. Phys.* **1971**, *54*, 1517. (c) Fritz, H. P.; Lüttke, W.; Stammreich, H.; Forneris, R. *Spectrochim. Acta* **1961**, *17*, 1068. (d) Schäfer, L.; Southern, J. F.; Cyvin, S. J. *Spectrochim. Acta* **1971**, *27A*, 1083.

Table 1. Center of Gravity (weighted average) of the Frequencies of the Key Bands of Benzene-Containing Complexes

| compound | $\nu(\text{CH})$ | $\nu(\text{CO})$ | $\nu(\text{CC})$ | C–C breathing | $\gamma(\text{CH})$ |
|--|------------------|------------------|------------------|---------------|---------------------|
| benzene | 3054 | | 1479 | 993 | 674 |
| (C ₆ H ₆) ₂ Cr | 3052 | | 1429 | 967 | 795 |
| [(C ₆ H ₆) ₂ Cr][PF ₆] | 3096 | | 1418 | 970 | 794 ^a |
| [(C ₆ H ₆) ₂ Cr][I] | 3044 | | 1437 | 969 | 795 |
| [(C ₆ H ₆) ₂ Cr][OH] | 3060 | | 1429 | 971 | 795 |
| (C ₆ H ₆)Cr(CO) ₃ | 3078 | 1897 | 1445 | 977 | 787 |
| [(C ₆ H ₆)Mn(CO) ₃][PF ₆] | 3089 | 2045 | 1456 | 985 | <i>b</i> |
| [(C ₆ H ₆)Mn(CO) ₃][I] | 3063 | 2047 | 1444 | 985 | |

^a Doubtful assignment: partially obscured by the very strong $\nu(\text{P–F})$ absorption. ^b Obscured by the very strong $\nu(\text{P–F})$ absorption.

**Figure 3.** Solid-state FT-IR (a) and Raman (b) spectra of $[(\eta^6\text{-C}_6\text{H}_6)\text{Mn}(\text{CO})_3]^+\text{I}^-$.

(7). The relevant frequency data, with suggested assignments, are reported in Table 2 SI and Table 3 SI of the Supporting Information.

We reiterate that, on the basis of previous observations on the spectra of metallocene complexes,¹ together with DFT calculations on complex **1** (vide infra), it is clear that the absence of kinematic coupling enables a separation of the spectra into selected regions, each corresponding to a “local” vibrational mode. For the internal modes of the benzene ligand they are the 3200–2800 cm⁻¹ region ($\nu(\text{CH})$ stretching modes), the 1600–1000 cm⁻¹ region ($\nu(\text{CC})$ stretching and in-plane $\delta(\text{CH})$ bending modes), and the 900–700 cm⁻¹ region (out-of-plane $\gamma(\text{CH})$ bending modes).¹⁶ Additionally, modes associated with the interaction between the benzene and the metal atom (usually at 400–100 cm⁻¹) and the vibrational modes of the other ligands (here CO groups), typically lying at 2100–1800 cm⁻¹ (CO stretch) and at 600–400 cm⁻¹ (M–CO stretch and M–C–O bend), have to be considered.

Internal Benzene Modes in the Complexes. We report in Table 1 the value of the center of gravity (weighted average) of the frequencies of some selected bands, together with the frequency of the so-called breathing mode of the ring, i.e., the totally symmetric in-plane mode involving all the C–C bonds. Figure 3 illustrates the IR and Raman spectra of complex **4b**.

Typically, $\nu(\text{CC})$ modes vary significantly moving from free to coordinated ligand. It is well known that the metal–benzene interaction¹⁷ involves σ -donation of electron density from the ligand π -orbitals to empty orbitals of the metal and π -back-donation from the populated metal orbitals to antibonding ligand

orbitals. Both these charge-transfer processes lower the electronic population of the benzene bonding MOs and, consequently, decrease the C–C bond order. This results in the frequency decrease of the, typically strong, infrared E₁ mode at ca. 1450 cm⁻¹¹⁸ and of the ring “breathing” A mode, dominant in the Raman spectrum near 1000 cm⁻¹ (see Table 2). The data show that these modes have a higher frequency in free benzene than in any of the benzene complexes. They show also that this effect is softened by the presence of the CO groups probably because of their great π -accepting capacity, which competes with and decreases the metal–benzene interaction. Finally, a minor—but evident—softening effect results from the positive charge of the complexes, which presumably also reduces the metal–benzene interaction. Noticeable is the sensitivity of the vibrational pattern to the nature of the metal–benzene bond. It shows a much greater sensitivity than do the values of other experimental parameters, such as the ¹³C NMR chemical shift²⁰ and the C–C bond distances.²¹

The symmetric out-of-ring plane bending mode of the H atoms appears as a strong infrared band in the 650–900 cm⁻¹ region. Two points should be emphasized. First, there is a large increase in frequency of this mode, moving from the free to the metal-bonded ligand. Second is the existence of differences within the same series of organometallic complexes. An analogous behavior has been discussed for Cp–M complexes¹ when the phenomena were mainly ascribed to the electrostatic interaction between the small positive charge on the H atoms and the variable charge on the ring. So, the first of the two effects probably reflects the electrostatic repulsion suffered by the hydrogen atoms when they are brought toward the metal atom.^{1,22}

The effect should vary with the ionic charge on the complex,^{1,23} but in the examples presented here, this cannot be demonstrated. For the ionic species, the 800–900 cm⁻¹ zone is obscured by the strong and broad absorption of the T_{1u} P–F stretching mode of the [PF₆]⁻ anion. Complex **4b** is the only one for which we could observe this band, but surprisingly, it shows a very low infrared intensity. This presumably demonstrates that the motion of the C–H bonds is sensitive to the positive charge distribution over the whole molecule.

Finally, the set of $\nu(\text{CH})$ bands in the 3000–3100 cm⁻¹ range is both a primary source of information on metal–ligand interactions and easily correlated with previous observations. If the center of gravity of the frequency of the band pattern is taken as reference, a clear observation is its increase with increase of the metal–benzene interaction; it is also closely correlated with the decrease in frequency of the $\nu(\text{C–C})$ modes, as reported above. Clearly, the decrease of the C–C electronic population, consequent upon metal–ring bonding, causes a strengthening of the C–H bonds²⁴ and the observed $\nu(\text{CH})$ increase.

(17) (a) Rayon, V. M.; Frenking, G. *Organometallics* **2003**, *22*, 3304. (b) Lyon, J. T.; Andrews, L. *J. Phys. Chem. A* **2005**, *109*, 431. (c) *Transition Metal Arene p-Complexes in Organic Synthesis and Catalysis Series: Topics in Organometallic Chemistry*, Vol. 7; Kündig, E. P., Ed.; Springer: Berlin, 2004; VIII 232, p 169.

(18) Calculation on several metal–benzene complexes has demonstrated that this frequency value is a good index of the C–C bond strength.¹⁹

(19) Chaquin, P.; Costa, D.; Lepetit, C.; Che, M. *J. Phys. Chem. A* **2001**, *105*, 4541.

(20) Graves, V.; Lagowski, J. J. *Inorg. Chem.* **1976**, *15*, 511.

(21) (a) Bailey, H. F.; Dahl, L. F.; Rees, B. *Inorg. Chem.* **1965**, *4*, 1314–1319. (b) Coppens, P. *Acta Crystallogr., Sect. B* **1973**, *29*, 2516.

(22) Langhoff, S. R. *J. Phys. Chem.* **1996**, *100*, 2819.

(23) Jaeger, T. D.; van Heijnsberger, D.; Klippenstein, S. J.; van Helden, G.; Meijer, G.; Duncan, M. A. *J. Am. Chem. Soc.* **2004**, *126*, 10981.

(24) Arrais, A.; Diana, E.; Gervasio, G.; Gobetto, R.; Marabello, D.; Stanghellini, P. L. *Eur. J. Inorg. Chem.* **2004**, 1505.

(15) (a) Adams, D. M.; Christopher, R. E.; Stevens, D. C. *Inorg. Chem.* **1975**, *14*, 1562. (b) Fritz, H. P.; Manchot, J. *Spectrochim. Acta* **1962**, *18*, 171. (c) Schäfer, L.; Begun, G. M.; Cyvin, S. J. *Spectrochim. Acta* **1972**, *26A*, 803. (d) English, A. M.; Plowman, K. R.; Butler, I. S. *Inorg. Chem.* **1982**, *21*, 338.

(16) The C–C–C ring deformation modes are not taken into account, because they appear as insignificant, weak bands in the 600–300 cm⁻¹ region.

Table 2. Frequency of the Chromium–Benzene Modes and Values of the Chromium–Benzene Stretching Force Constants

| complex | Cr–benzene stretching | | benzene–Cr–benzene tilting | | force constant (mdyn/Å) | |
|---|-----------------------|-----------------|----------------------------|-----------------|-------------------------|----------|
| | A _{1g} | A _{2u} | E _{1g} | E _{1u} | <i>f</i> | <i>k</i> |
| Bz ₂ Cr ^a | 274 | 459 | 342 | 491 | 2.94 | 0.52 |
| [Bz ₂ Cr] ⁺ [I] [−] | 282 | 418 | 336 | 466 | 2.82 | 0.84 |
| [Bz ₂ Cr] ⁺ [OH] [−] | 275 | 420 | 340 | 465 | 2.75 | 0.73 |
| [Bz ₂ Cr] ⁺ [PF ₆] [−] | 272 | 425 | 329 | 463 | 2.74 | 0.66 |
| BzCr(CO) ₃ ^b | 295 | | 330 | | 2.54 | |
| [Bz ₂ Cr] ⁺ (DFT calc) | 272 | 396 | 326 | 486 | 2.60 | 0.80 |

^a Infrared band at 427 cm^{−1}, probably ascribed to the benzene–Cr–benzene bending mode. ^b Infrared band at 423 cm^{−1}, probably ascribed to the benzene–Cr bending mode.

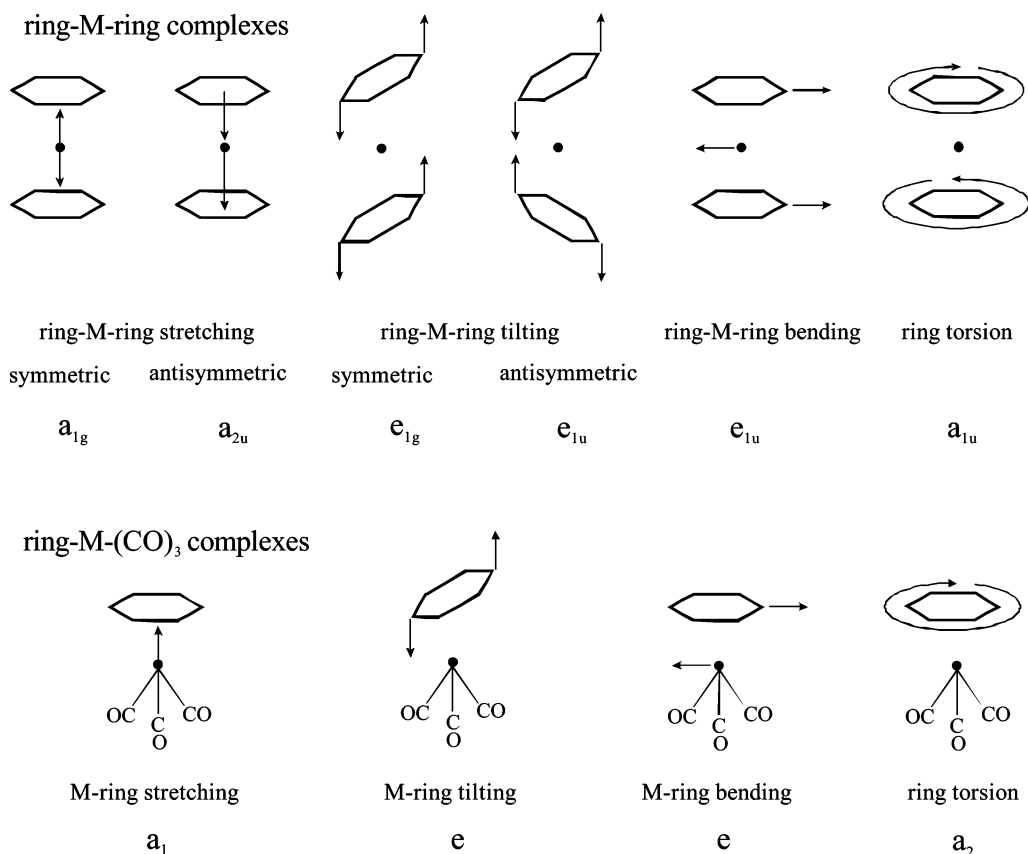


Figure 4. Sketches of the modes arising as a result of the bonding between the metal and the ring, in the sandwich complexes (D_{6h} symmetry) and in the ring $M(\text{CO})_3$ complexes (C_{3v} symmetry).

Metal–Benzene Modes. Figure 4 illustrates the modes arising as a result of the bonding between the metal and the ring, together with appropriate symmetry correlations between the single-ring complexes (C_{3v} symmetry) and the sandwich complexes (D_{6h} symmetry).

The frequencies of these modes lie in the 500–250 cm^{−1} region. The DFT calculations help the assignment and show that the coupling between these modes and other modes with similar energies, such as the out-of-plane ring deformation modes, is quite low. Table 2 lists the most probable assignments together with the value of the M–ring force constant calculated by a two-body or three-body approximation. The values are in the same range as those reported for metallocene complexes,¹ being lower than those of the most stable metallocenes (e.g., FeCp₂, [CoCp₂⁺]), but higher than those of the unstable, very reactive metallocenes (e.g., MgCp₂, VCp₂, NiCp₂). Bz₂Cr shows a somewhat greater value than the corresponding cation, suggesting a greater M–Bz bond strength, an interpretation supported by the reported M–Bz distances (1.591 vs 1.612 Å).^{3,25}

CO Stretching Modes. The $\nu(\text{CO})$ modes (2100–1800 cm^{−1} range) are typical and give rise to IR and Raman features that are very sensitive to the ionic charge of the compounds,²⁶ showing a ca. 150 cm^{−1} upshift from neutral (ca. 1900 cm^{−1}) to positively charged (ca. 2045 cm^{−1}) complexes. The band pattern in solution is very simple, two infrared and two coincident Raman bands, in conformity with the C_{3v} symmetry. In the solid state the molecular compound **3** shows a much more complex behavior, as previously described,²⁷ due to (intermolecular) coupling between the molecular CO modes (factor group effects). Noteworthy is the large shift to lower frequencies (ca. 50 cm^{−1}) of the center of gravity (cog) of the bands obtained for the solid compared with the solution bands. There could be many explanations for this, but one that surely makes a

(25) Jellinek, F. *J. Organomet. Chem.* **1963**, *1*, 43.

(26) De La Cruz, C.; Sheppard, N. *J. Mol. Struct.* **1990**, *224*, 141.

(27) (a) Kettle, S. F. A.; Buttery, H. J.; Keeling, G.; Paul, I.; Stamper, P. *J. Chem. Soc. A* **1969**, 2077 (b) Kettle, S. F. A.; Buttery, H. J.; Keeling, G.; Paul, I.; Stamper, P. *Discuss. Faraday Soc.* **1969**, *47*, 48. (c) Kettle, S. F. A.; Buttery, H. J.; Keeling, G.; Paul, I.; Stamper, P. *J. Chem. Soc. A* **1970**, 471. (d) Kettle, S. F. A.; Buttery, H. J.; Paul, I. *J. Chem. Soc., Dalton Trans.* **1974**, 2293.

contribution is that it is connected with the presence of factor group effects. Factor group coupling is usually, for simplicity, pictured as resulting from molecules within the same unit cell (here, there are just two such molecules, inter-related by a center of symmetry). In reality, of course, any one molecule vibrationally couples with all of those surrounding it. Although this additional coupling must give rise to frequency changes, it cannot be seen as a splitting because of the $k = 0$ limitation. That is, the wavelength of the probe, infrared or Raman, radiation is so much greater than typical intermolecular distances that the only modes that can be seen are those in which translationally related molecules vibrate in phase. But the “invisible” coupling will lead to a change in the observed frequency of the corresponding features. Nonetheless, the size of the shift, in comparison with the factor group splitting, is such that some other contributing mechanisms cannot be excluded, such as the hydrogen interaction with the oxygen atoms. The structure²¹ reveals some $\text{CH}\cdots\text{OC}$ distance values, between 2.60 and 3.20 Å, which lie in the range of typical $\text{O}\cdots\text{H}$ bonds.

In the ionic complexes **4**, in contrast, the solution and solid-state patterns are almost identical; the frequency values do not depend on the counteranion. Evidently, in the crystals the organometallic cations are “diluted” by the anion frame and well separated from each other, much as occurs in solution, preventing any coupling between neighboring $(\text{CO})_3$ units.

Intermolecular Interaction: The Blue-Shift Hydrogen Bond. The $\nu(\text{CH})$ pattern serves as a sensitive sign of intermolecular interactions and is both significant and interesting.²⁸ The C–H bonds are, effectively, “external” to the complex and directed toward neighboring systems, so that vibrational interference can occur with them. One immediate observation is that the pattern is always much more complicated than that expected on the basis of the molecular symmetry (see, for example, complex **3**), indicating that site group or factor group effects are relevant. No less important is a possible hydrogen bond between the CH groups and adjacent electronegative atoms in the crystal network. A possible candidate is the O atom of the CO group, data on which have been reported for $[\text{Co}(\text{CO})_4]^-$.²⁹ Clearly, no such hydrogen bonding occurs for **4a** and **4b**, as the CO vibrational characteristics are essentially the same for solution and crystal. However, important interactions are evident between CH groups and the counteranions $[\text{PF}_6]^-$ and $[\text{I}]^-$. Of these, the $\nu(\text{CH})$ cog is significantly higher for **4a** than for **4b**. If we take complex **3** as reference (it has no anion and so no intermolecular interaction with one), the $\nu(\text{CH})$ cog of **4a** is higher by 10 cm^{-1} and, by the same criterion, the $\nu(\text{CH})$ cog of **4b** is lowered. Even more convincing is a comparison between the solution and the solid-state infrared spectra of **4a** and **4b**. As Figure 5 shows, the two spectra in solution are superimposable, as expected since they are both the $\nu(\text{CH})$ pattern of the $[\eta^6\text{-C}_6\text{H}_6\text{Mn}(\text{CO})_3]^+$ cation and interaction with their anions is negligible. In the spectra of the crystals, the $\nu(\text{CH})$ pattern is clearly shifted toward higher frequency for **4a** and toward lower frequency for **4b**. These are typical cases of blue- and red-shifted hydrogen bond vibrations, very similar to those that we have previously reported for ferrocenium and cobaltocenium salts.³⁰

In simple systems, experimental evidence for a blue-shifted H-bond vibration seems to be limited to few examples of adducts

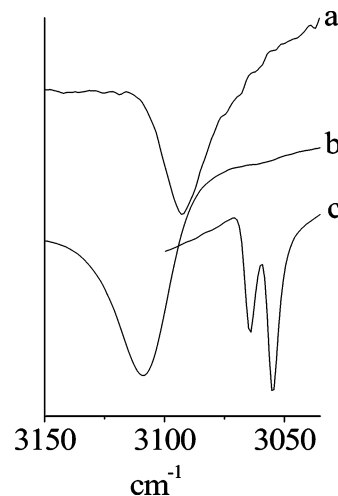


Figure 5. FT-IR spectra of $[\eta^6\text{-C}_6\text{H}_6\text{Mn}(\text{CO})_3]^+$ cation (CH_3CN solution, a), $[(\eta^6\text{-C}_6\text{H}_6)\text{Mn}(\text{CO})_3]^+[\text{PF}_6]^-$ (KBr pellet, b), and $[(\eta^6\text{-C}_6\text{H}_6)\text{Mn}(\text{CO})_3]^+[\text{I}]^-$ (KBr pellet, c), showing blue- and red-shift of the $\nu(\text{CH})$ stretching.

between proton donors with C–H bonds and proton acceptors such as π -systems³¹ or oxygen lone pairs.³² In contrast, it is surprisingly common in the crystal phases of organometallic ionic complexes, which may have a wide variety of (C_nH_n) ring ligands and equally varied counteranions.

It should be very significant to compare the $\nu(\text{CH})$ shift with the measured C–H distance. To do that, the location of the hydrogen atoms in the crystal frame should be carefully determined, which requires neutron diffraction experiments on single crystals at low temperature, possibly by means of D labeling. A very accurate H location is really necessary, as many theoretical calculations on molecular adducts showing blue- and red-shifts indicate that a $\Delta\nu(\text{CH})$ of ca. $20\text{--}30\text{ cm}^{-1}$ compares with a variation of few mÅ on the CH distance.³³ Unfortunately, the structures of organometallic salts available at the moment report approximate H position, sometimes given by assuming a standard C–H distance.^{3–5}

(B) Tropilium Salts. The high symmetry of the tropilium ion (D_{7h}) limits the total number of vibrationally active modes to four infrared and seven Raman (Appendix in SI collects the appropriate details). Consequently, the infrared and Raman spectra are very simple, as illustrated as long ago as 1956.³⁴ This paper reports also the first assignment, later revised by Sourisseau,³⁵ who performed a force field analysis on the ion. More recently, DFT calculations using a variety of basis sets have been performed.³⁶ As an independent assessment of the interpretation of the spectra, we have calculated them using the DFT method. The optimized structure with $d_{\text{C-C}} = 140.06\text{ pm}$ and $d_{\text{C-H}} = 109.4\text{ pm}$ agrees well with the experimental values

(31) Reimann, B.; Buchhold, K.; Vaupel, S.; Brutschy, B.; Havlas, Z.; Špirko, V.; Hobza, P. *J. Phys. Chem. A* **2001**, *105*, 5560.

(32) (a) van der Veken, B. J.; Herrebout, W. A.; Szostak, R.; Shchepkin, D. N.; Havlas, Z.; Hobza, P. *J. Am. Chem. Soc.* **2001**, *123*, 12290. (b) Delanoye, S. N.; Herrebout, W. A.; van der Veken, B. J. *J. Am. Chem. Soc.* **2002**, *124*, 11854. (c) Blatchford, M. A.; Raveendran, P.; Wallen, L. S. *J. Am. Chem. Soc.* **2002**, *124*, 14818. (d) Vaz, P. D.; Ribeiro-Claro, J. A. *J. Raman Spectrosc.* **2003**, *34*, 863.

(33) (a) Alabugin, I. V.; Manoharan, M.; Peabody, S.; Weinhold, F. *J. Am. Chem. Soc.* **2003**, *125*, 5973. (b) Rhee, S. K.; Kim, S. H.; Lee, S.; Lee, J. Y. *Chem. Phys.* **2004**, *297*, 21. (c) Hobza, P.; Havlas, Z. *Chem. Rev.* **2000**, *100*, 4253.

(34) Fateley, W. G.; Curnutte, B.; Lippincott, E. R. *J. Chem. Phys.* **1956**, *1471*.

(35) Sourisseau, C. *Spectrochim. Acta* **1978**, *34A*, 881.

(36) Bandyopadhyay, I.; Manogaran, S. *J. Mol. Struct. (THEOCHEM)* **1998**, *432*, 33.

(28) Arrais, A.; Boccaleri, E.; Croce, G.; Milanese, M.; Orlando, R.; Diana, E. *CrystEngComm* **2003**, *5*, 388.

(29) Bockman, T. M.; Kochi, J. K. *Am. Chem. Soc.* **1988**, *110*, 1294.

(30) Diana, E.; Stanghellini, P. L. *J. Am. Chem. Soc.* **2004**, *126*, 7418.

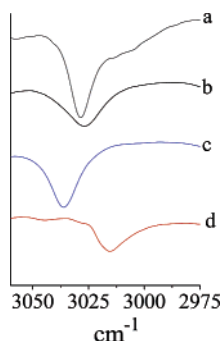


Figure 6. FT-IR spectra of $\text{Tp}^+[\text{PF}_6]^-$ (CH_3CN solution, a), [18-dibenzo-crown-6·(Tp^+)] $[\text{PF}_6]^-$ (KBr pellet, b), $\text{Tp}^+[\text{PF}_6]^-$ (KBr pellet, c), and $\text{Tp}^+[\text{SbCl}_6]^-$ (KBr pellet, d), showing blue- and red-shift of the $\nu(\text{CH})$ stretching.

$d_{\text{C}-\text{C}} = 139.9$ pm and $d_{\text{C}-\text{H}}$ (estimated) = 109.9 pm, giving us confidence in the reliability of our calculated spectra. In the present work, we have measured the spectra (both in the solid state and in solution) of the Tp^+ salts of the $[\text{PF}_6]^-$ and the $[\text{SbCl}_6]^-$ anions. All these data are collected and compared in Table 4 SI.

The assignment of the bands is generally agreed and is supported by the DFT calculations. It is important to recognize that the modes whose frequencies lie between 1600 and 900 cm^{-1} are all assignable to coupled CC-stretching and CH-in-plane deformations. An exception is the strong Raman band at 868 cm^{-1} , which is a pure $\nu(\text{CC})$ mode, the totally symmetric elongation of all C–C bonds (the ring breathing mode). The appearance of two strong infrared bands in the 660–620 cm^{-1} range where just one is expected (the $\gamma(\text{CH}) A_2''$ bending mode) can be explained with the help of the DFT calculations, which suggest that this mode is the one with lowest frequency and highest intensity. The other band is possibly a combination of ring deformation modes, as has previously been suggested.³⁴ An interpretation of the second band as due to the presence of impurity Tp^+X^- species (perhaps Tp^+Cl^- in the $\text{Tp}^+\text{PCl}_6^-$)³⁵ can be excluded, because the band pair appears to be a common feature of all tropilium salts.

The majority of the Tp^+ vibrations lead to unexceptional bands with the exception of the $\nu(\text{CH})$ modes, which deserve more attention. The solution spectra are very simple: two Raman (A_1' and E_2') and one infrared (E_1') band, corresponding to the active modes. The spectra of the solids exhibit a new medium-weak Raman band at 3070 cm^{-1} , presumably the silent E_3' mode. There are also some weak infrared bands at a frequency greater than 3100 cm^{-1} , probably overtones and/or combinations of normal modes, all these gaining some intensity by the reduction of symmetry in the crystal. Consider the E_1' fundamental mode, a feature of medium intensity in solution. A frequency shift is observed, varying with media and anion (Figure 6). It clearly resembles that reported above for benzene complexes. The value in solution (3028 cm^{-1}) does not depend on the anion, but increases to 3037 cm^{-1} in the solid-state spectrum of the $[\text{PF}_6]^-$ salt and decreases to 3015 cm^{-1} when the spectrum of the $[\text{SbCl}_6]^-$ salt is measured. This is clear evidence of blue- and red-shifts associated with hydrogen bonds in the same Tp^+X^- series. The different shifts presumably reflect subtle differences in the interaction between the Tp^+ proton donor and the X^- proton acceptors. Support for this interpretation comes from the spectrum of the crystalline $[\text{PF}_6]^-$ salt of the tropilium cation complexed by the crown ether (dibenzo-18-crown-6). The corresponding E_1' mode shows a frequency at 3027 cm^{-1} , the same value as that recorded in solution.

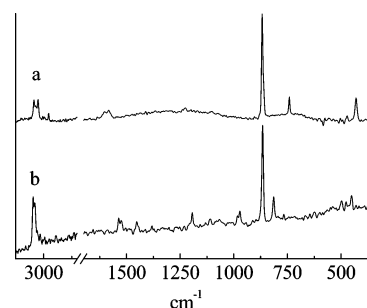


Figure 7. Solid-state Raman spectra of $\text{Tp}^+[\text{PF}_6]^-$ (a) and $[\text{TpCr}(\text{CO})_3]^+[\text{BF}_4]^-$ (b).

Clearly, the crown ether acts as a spacer, as do the solvent molecules in solution, preventing any contact between the cation/anion pair. This contact, even if less evident, is also signaled by the C–H out-of-plane bending mode. The highest frequency value (642 cm^{-1} for the crystalline $[\text{PF}_6]^-$) occurs with the highest C–H bond stretch blue-shift. Conversely, the lowest frequency value (632 cm^{-1} for crystalline $[\text{SbCl}_6]^-$) is associated with the largest red-shift for the C–H bond stretch. It is to be noted that the frequency in solution is intermediate (639 cm^{-1}).

(C) Tropilium Complexes. Formally, the symmetry of the two tropilium complexes **6** and **7** is very low (C_s or C_1 ; see Figure 2). Nonetheless, the spectral patterns of the internal tropilium modes are quite simple and very similar to those of the tropilium salts (Figure 7). It can reasonably be assumed that the local C_7 symmetry is dominant in the complexes. The values of the frequencies of the main vibrational modes, together with the relevant assignments, are listed in Table 5 SI.³⁷

Coordination of the ligand to the metal changes the frequency of the key modes of the isolated ligand. The changes follow those that we have previously detailed for the case of benzene; that is, the C–C bond stretch moves to lower frequency and the C–H bond out-of-plane bend moves toward higher frequency. More intriguing is, as usual, the behavior of the C–H stretch, which exhibits two opposite trends, i.e., a small shift to lower frequency for the neutral complex **7** and a significant higher frequency shift for the ionic complex **6**. This behavior can be easily understood by recognizing that the reference system, the free tropilium ligand, is a cation and not a neutral molecule like benzene. So, two effects are simultaneously present and give rise to opposite results: (i) coordination to the metal, which increases the average $\nu(\text{CH})$ frequency, and (ii) a decrease of the positive molecular charge, which decreases the frequency. The ionic complex **6**, with the same charge as the reference Tp^+ cation, behaves as expected when effect (i) is operating, whereas in the Mn complex both the effects are present and, more or less, compensate.

The $\nu(\text{CO})$ pattern is worthy of attention. The cog of complex **6** is greater than that of complex **7** by ca. 60 cm^{-1} , the expected increase when comparing a neutral system with one with a positive charge (Table 3). Particularly interesting is the frequency shift to higher wavenumber of the solution compared to the solid-state spectra. The shift is small (4–5 cm^{-1}) for complex **7** and simply reflects the different media, but it is significantly greater for the ionic complex **6** (ca. 15 cm^{-1}). This could have the same origin as discussed earlier, a translationally independent coupling of CO groups in the crystal lattice. A contribution could also arise from long-range interactions in the crystal lattice. In the present case there could be a C–O···H–C

(37) (a) Harvey, P. D.; Butler, I. S.; Gilson, D. F. R. *Inorg. Chem.* **1987**, 26, 32. (b) Howard, J.; Graham, D. *Spectrochim. Acta, Part A* **1985**, 41A, 815.

Table 3. Frequency and Assignment of the $\nu(\text{CO})$ Modes of the Tropilium Complexes

| complex | medium | symmetric mode | antisymmetric mode |
|--|-------------|-----------------------|------------------------|
| [TpCr(CO) ₃][BF ₄] | solid state | 2059 R 2058 IR | 2016 R 2026/2006 IR |
| | solution | 2071 IR | 2032 IR |
| TpMn(CO) ₂ Br | solid state | 2008 R ca. 2008 IR | 1953 R ca. 1959 IR |
| | solution | 2013 IR | 1962 IR |

hydrogen bond, which would weaken the C–O bond and strengthen the C–H.

Finally, only one band can be unequivocally assigned to the vibrational modes expected for the metal–tropylium bond, i.e., the strong Raman band at 305 cm⁻¹ in complex **6**, clearly the metal–ligand stretching vibration. An approximate force constant value can be calculated (2.99 mdyn/Å), which is comparable to those associated with metal–benzene stretches.

Conclusion

There is no doubt that in the formation of a crystal phase the physical packing requirements will mean that groups will be forced into unusual situations with respect to each other.³⁸ In that each atom in a crystal is at equilibrium, it is to be expected that some unusual interactions will be brought into existence and can be revealed by some suitable technique. It would appear that the hydrogen bond blue-shift is one of the few such novel interactions that have been revealed³⁹ and that the vibrational spectroscopy seems to provide an excellent probe for such a weak but unusual interaction.

The spectroscopic analysis presented here for many transition metal complexes containing C_nH_n aromatic rings has confirmed that weak intermolecular interaction between the ring and different functional groups of such complexes begins to appear quite regularly in the solid state of these systems. Other systems are expected to contain evidence of yet other weak intermolecular bonds or repulsions, such as situations in which electropositive and electronegative elements are forced into close proximity.

Vibrational IR and Raman spectroscopy appears an ideal technique to reveal and “quantify” these phenomena. The assignment of the vibrational normal modes (of both the free rings and the related complexes) is important to understand the

(38) Braga, D.; De Leonardis, P.; Grepioni, F.; Tedesco, E.; Calhorda, M. J. *Inorg. Chem.* **1998**, *37*, 3337.

(39) (a) Zierkiewicz, W.; Jurecka, P.; Hobza, P. *ChemPhysChem* **2005**, *6*, 609. (b) Saar, B. G.; O'Donoghue, G. P.; Steeves, A. H.; Toman, J. W. *Chem. Phys. Lett.* **2006**, *417*, 159. (c) Karpfen, A.; Kryachko, E. S. *J. Phys. Chem. A* **2005**, *109*, 8930.

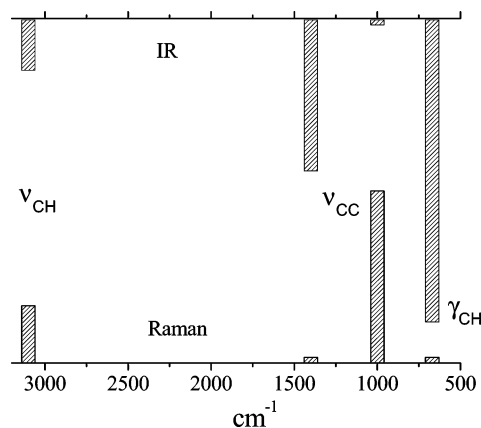


Figure 8. Schematic pattern of the main vibrational modes of a $\pi(\text{C}_n\text{H}_n)$ ring bonded to a metal atom.

difference between the solution and the solid state. In addition, a comparison between the vibrations of the free and metal-coordinated rings enables an understanding of the effect of the coordination on the ring electronic charge distribution. The complement represented by theoretical DFT data has been very useful in facilitating the assignments, especially in “doubtful” cases, or when the presence of “vibrationally active” counterions makes a correct assignment of some ring modes difficult.

The data collected have allowed a characterization of a spectroscopic pattern, common to any $\pi\text{-C}_n\text{H}_n$ ring ($n = 5-7$) bonded to a metal atom. This pattern is schematically illustrated in Figure 8. The features reported in both infrared and Raman spectra represent the key bands of the ring, in the sense that they define the presence of this ligand (a vibrational “fingerprint”). Anyway, a more peculiar property of these bands is their sensitivity (in terms of band frequency and intensity) to any change of the electronic distribution in the complex and to any change of the surroundings around the complex, thus being a primary test of the presence of weak interactions in the crystal frame.

Acknowledgment. This work has been supported by the Università di Torino through a Cooperation Agreement with the University of East Anglia (E.D. and S.F.A.K.).

Supporting Information Available: The SI includes details on the tropylium vibrational modes (Appendix), a list of the vibrational modes of the free and coordinated benzene ligand (Table 1 SI), and the frequencies and assignments of the (benzene)₂Cr complexes (Table 2 SI), the (benzene)M(CO)₃ complexes (Table 3 SI), the tropylium salts (Table 4 SI), and the tropylium complexes (Table 5 SI). This material is available free of charge via the Internet at <http://pubs.acs.org>.

OM060431B